Nano Energy 90 (2021) 106579

Contents lists available at ScienceDirect

Nano Energy

journal homepage: www.elsevier.com/locate/nanoen

Trace oxophilic metal induced surface reconstruction at buried RuRh cluster interfaces possesses extremely fast hydrogen redox kinetics

Yujia Cui [a,1], Zihan Xu [a,1], Ding Chen [b,1], Tingting Li [a], Hao Yang [a], Xueqin Mu [a], Xiangyao Gu [a,c], Hong Zhou [a], Suli Liu [a,*], Shichun Mu [b,d,**]

[a] Key Laboratory of Advanced Functional Materials of Nanjing, Nanjing Xiaozhuang University, Nanjing 211171, China
[b] State Key Laboratory of Advanced Technology for Materials Synthesis and Processing, Wuhan University of Technology, Wuhan 430070, China
[c] Guangxi Key Laboratory of Low Carbon Energy Materials, Guangxi Normal University, Guilin 541004, China
[d] Foshan Xianhu Laboratory of the Advanced Energy Science and Technology Guangdong Laboratory, Xianhu hydrogen Valley, Foshan 528200, China

ARTICLE INFO

Keywords:
Hydrogen oxidation
Oxophilic metal
Ru (Rh) clusters
Atom reconstruction

ABSTRACT

Developing high-efficiency electrocatalysts is the key to generating and consuming hydrogen by accelerating the reaction kinetics of the hydrogen oxidation and evolution reactions (HOR/HER). Although the kinetics process of the adsorbed intermediates (H_{ad})-water-oxophilic metal has been investigated in the alkaline media, the hydroxyl species (H_{ad} or OH^- or OH_{ad})-activity relationship for oxophilic metal alloy electrocatalysis during multiple HOR and HER processes is still unclear. In this regard, our density functional theory (DFT) calculation results show that, due to partial substitution of Ru (Rh) clusters at buried interfaces by oxophilic-metal (OM) species, the long-range order of Ru (Rh) clusters surface atoms can be broken, and then the active atom reconstruction at buried interfaces is triggered, which decreases the oxidation intermediates of Ru (Rh) and gives rise to the increased activity for alkaline HER/HOR. At the same time, an OH^--adsorption promoter forms, also favorable for OER. Encouraged by the first-principles calculation results, an ultralow-loaded OM species (0.13 wt % Co, 0.23 wt% Mn, 2.4 wt% Cr or 1.3 wt% Fe) incorporated RuRh cluster (RuRh-OM) catalyst is built by a mixed-solvent strategy. Impressively, after incorporating OM (Co; Mn; Cr and Fe), these catalysts exhibit higher HOR activity than pristine RuRh and commercial Pt even at higher potentials in 0.1 M KOH solutions, which outperforms most reported HOR catalysts and ~ 2 times higher than that of commercial Pt. Meanwhile, RuRh-Co also exhibits the highest HER activity among all reported Ru-based HER catalysts, and greatly improved OER and overall water spitting performances in alkaline solutions (1 M KOH for HER and overall water spitting, 0.1 M KOH for OER), exceeding RuRh and commercial noble metal catalysts.

1. Introduction

For electrocatalysis, hydrogen evolution and oxidation reactions (HER/HOR) as hydrogen redox, as well as oxygen evolution reaction (OER), are three important reactions for regenerative fuel cells, metal-air batteries and large-scale hydrogen production from water electrolysis [1,2]. Traditionally, platinum (Pt)-based catalysts, which have a slightly negative hydrogen absorption energy and minimum overpotential, is considered to be the best-known catalyst for HER/HOR [3–5]. However, compared with the acid media environment, the HOR kinetics of Pt-group metals are often ~100 times slower in alkaline solutions owing to the unsuitable adsorption/desorption capacity of the reaction intermediates (H*/OH*) [5]. Thus, the main strategy for improving alkaline HOR is adjusting the OH species binding energy (OHBE) of catalysts on account of bifunctional theory, involving introduction of oxophilic element [6,7]. Furthermore, both HER and HOR process in alkaline media involve the same particular intermediate species (H*/OH*) [8–10]. Accordingly, research efforts are increasingly devoted to designing efficient HOR/HER electrocatalysts with optimal OHBE. In addition, Ru-OM (OM = oxophilic metal) alloys exhibited

* Corresponding author.
** Corresponding author at: State Key Laboratory of Advanced Technology for Materials Synthesis and Processing, Wuhan University of Technology, Wuhan 430070, China.
E-mail addresses: niuniu_410@126.com (S. Liu), msc@whut.edu.cn (S. Mu).
[1] Y. J. Cui, Z. H. Xu, and D. Chen contributed equally to this work.

https://doi.org/10.1016/j.nanoen.2021.106579
Received 10 June 2021; Received in revised form 23 September 2021; Accepted 25 September 2021
Available online 29 September 2021

enhanced OER activity in alkaline electrolytes [11,12]. Nevertheless, extreme scarcity, and high dosage and cost, have driven efforts to exploit high-efficiency Pt-group HOR catalysts with greatly decreased amount toward commercial applications in alkaline media.

As state-of-the-art Pt-free cathode catalysts, Ru-based materials are always highly active for the electrocatalytic OER/HER due to similar properties to Pt while 10 times lower in price than Pt [13–15]. Meanwhile, as a member of Pt-group metals, rhodium (Rh) is extensively used in various catalytic reactions [16,17]. In fact, Ru(Rh) has a very small ΔG_{H^*} close to that of Pt and thus can be used as an alternative to Pt [17]. However, Ru-based catalysts seem to be an inappropriate option because of easy oxidization, making it difficult to maintain an oxide-free surface for bonding with intermediates [14]. This results in rapidly decreasing HOR activity under a relatively high potential range in an alkaline environment. Recently, the "oxophilic effect" and/or electronic effects have enabled the oxidative removal of adsorbed hydrogen, leading to increased HOR activity [6,7,18,19]. In contrast, under alkaline conditions, alloying Ru(Rh) with Co, Ni, and Fe significantly enhanced the OER activity by in-situ formation of an oxide layer [11,12,20]. Hence, an ideal Ru-based HER/HOR catalyst shall possess optimal surface with an oxide layer, allowing an optimum anti-oxidation capacity in alkaline environments under a relatively high potential range.

In principle, oxophilic metals introduced RuRh alloy clusters at buried interfaces are easy to be reconstructed or melts in the defect areas and optimizes the diversity of adsorption sites, benefiting their multiple HOR electrocatalysis. Here, to better understand the hydroxyl species (H_{ad} or OH^- or OH_{ad})-activity relationship and predict materials with promising HER/HOR activity, several different 3d metal doped RuRh structural models were firstly constructed and optimized by the DFT simulations based on our previous report under alkaline conditions [21]. The results shown that the addition of OM (OM = Co; Mn; Cr and Fe) to RuRh can decrease the hydrogen adsorption energy (ΔG_H), increasing the HOR activity. Thus, based on these doping models, we propose a general doping strategy, in which the ultralow-loaded 3d metal species regulates the *d*-band center of RuRh clusters and hence gets better overall catalytic performance. Accordingly, ultralow-loaded oxophilic metal species (OM = Co; Mn; Cr; and Fe) incorporated RuRh clusters are designed and built for HOR. To note, the optimized RuRh-Co demonstrates excellent HOR/HER performance in alkaline solutions activities. The results shed light onto the effect of "oxophilic effect" on key atom-level descriptors for catalysis.

2. Results and discussion

Density functional theory (DFT) calculations were applied to investigate the high anti-oxidation performance of RuRh-OM (OM = Co; Mn; Cr and Fe) catalysts (Fig. 1a and S1). As shown in Fig. 1b, by comparing different Ru or Rh 3d orbital from projected partial density of states (PDOSs), the PDOS structure changes significantly from RuRh to RuRh-OM, which means that the formation of RuRh-OM can lead to the *d*-band widening and *d*-band center shifting upward toward the Fermi level. Such as, compared with the pure RuRh clusters, the upshift of the *d*-band center increases the adsorption of RuRh-Co to intermediate species, conducive to intermediate species desorption and indicative of the improvement of HOR activity [22,23]. Generally, the HOR in alkaline media undergoes Volmer-Heyrovsky or Volmer-Tafel mechanism [24,

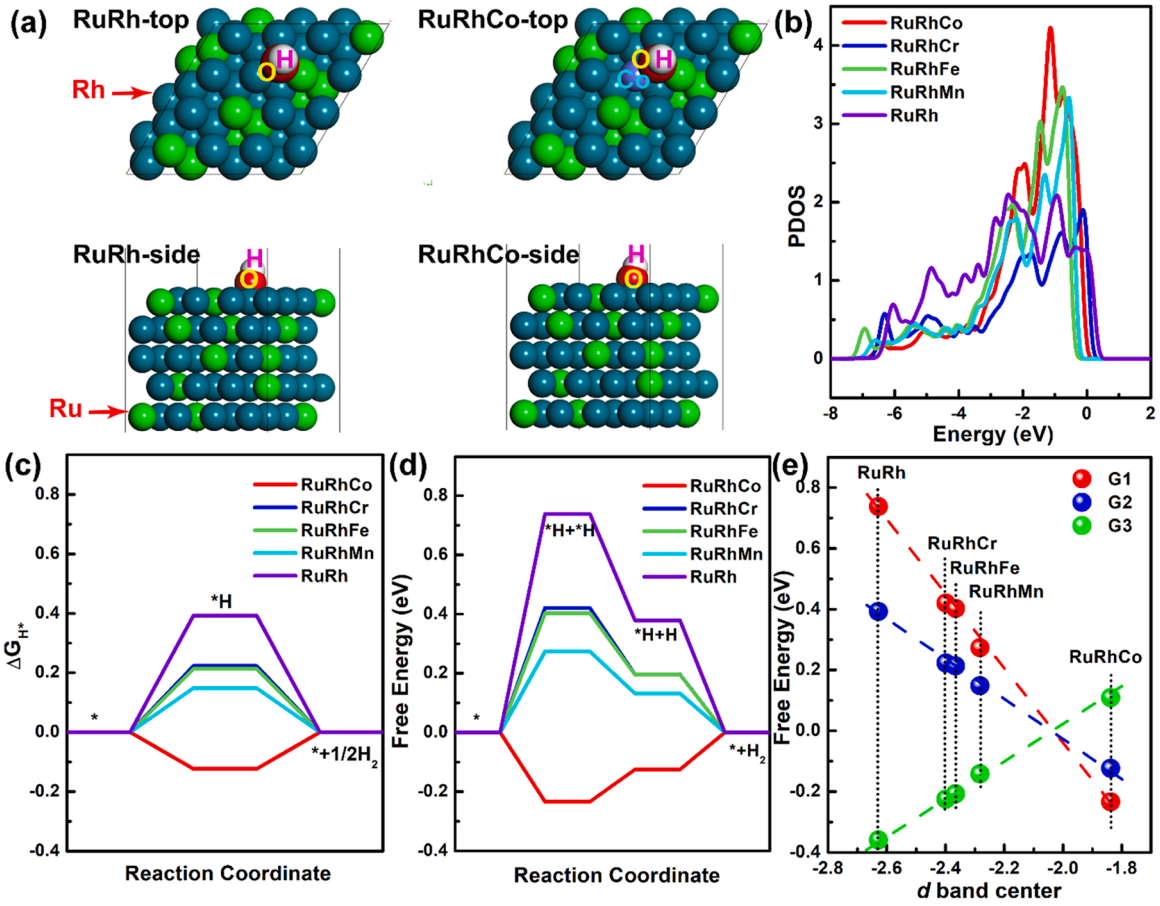

Fig. 1. Side and Top views of RuRh-Co catalysts models. Blue: Rh; Green: Ru. (b) Projected density of states in RuRh and RuRh-OM (OM = Co, Mn, Cr, and Fe) catalysts. (c)Free energy differences for HOR in alkaline medium on RuRh and RuRh-OM, respectively. (d) Free energy differences for HOR on RuRh and RuRh-OM, respectively. (e) Correlation between the energy barrier for water formation and *d*-band center on RuRh and RuRh-OM (OM = Co, Mn, Cr, and Fe) catalysts (G1: $H_2 + 2 * \rightarrow 2\,H_{ad}$; G2: $H_2 + OH^- + *\rightarrow H_{ad} + H_2O + e$; G3: $H_{ad} + OH^- \rightarrow H_2O + e + *$).

25], Thus, the alkaline HOR is normalized by the reactivity of intermediate species (H*/OH*), i.e., the intermediate adsorption energy (ΔG) can affect the HOR rate. In this work, through substituting partial Ru (Rh) clusters with oxophilic-metal species at buried interfaces, it causes the formation of OH_{ads} on the oxophilic-metal surface, increasing the OH species binding energy (OHBE) and enhances the HOR kinetics. Fig. 1c and d shows that the HOR activities are in the order of: RuRh (0.39 eV) < RuRh-Cr (0.22 eV) < RuRh-Fe (0.21 eV) < RuRh-Mn (0.15 eV) < RuRh-Co (0.12 eV). Meanwhile, Fig. 1e shows the relationship between the ΔG and the *d*-band center of RuRh-OM (OM = Co, Mn, Cr and Fe) catalysts. The large ΔG value for the bare RuRh surface indicates too strong adsorption to intermediate species, unfavorable for the reaction [10,26]. Undoubtedly, the addition of OM to RuRh decreases the ΔG, thus increasing the HOR activity. Meanwhile, the alkaline environment favors $OM(OH)_X$ species, enhancing OER activity [27]. Overall, we also support the theory that a bifunctional mechanism where RuRh is mitigating dissociative H adsorption and OMO_x provides the OH^-, facilitating the overall HER/HOR/OER kinetics in alkaline media.

Inspired by the DFT calculation results, RuRh-OM (OM = Co, Mn, Cr, and Fe) was constructed by a mixed-solvent strategy, in which $RhCl_3.3\,H_2O$, $RuCl_3{\cdot}xH_2O$ and $CoCl_2.6\,H_2O$ ($MnCl_3$, $Fe(acac)_2$, $Cr(acac)_2$) were selected as the metal precursors (Fig. 2a). As example of RuRh-Co, its morphology and structure were characterized by transmission electron microscopy (TEM). As shown in Fig. 2b and c, RuRh-Co exhibits a porous multipod-like nanostructure, which is beneficial for enhancing the electrochemical performance by increasing surface area and boosting mass transfer. When amplifying the TEM images, the porous sheet-like profile with a high density of low-coordinated atomic step can be observed (Fig. 2d and S2), which breaks the long-range order of Ru (Rh) cluster surface atoms and induces the active atom reconstruction at buried interfaces, which proves our previous inference [22, 28]. Also, RuRh-Co shows a high density of low-coordinated atomic

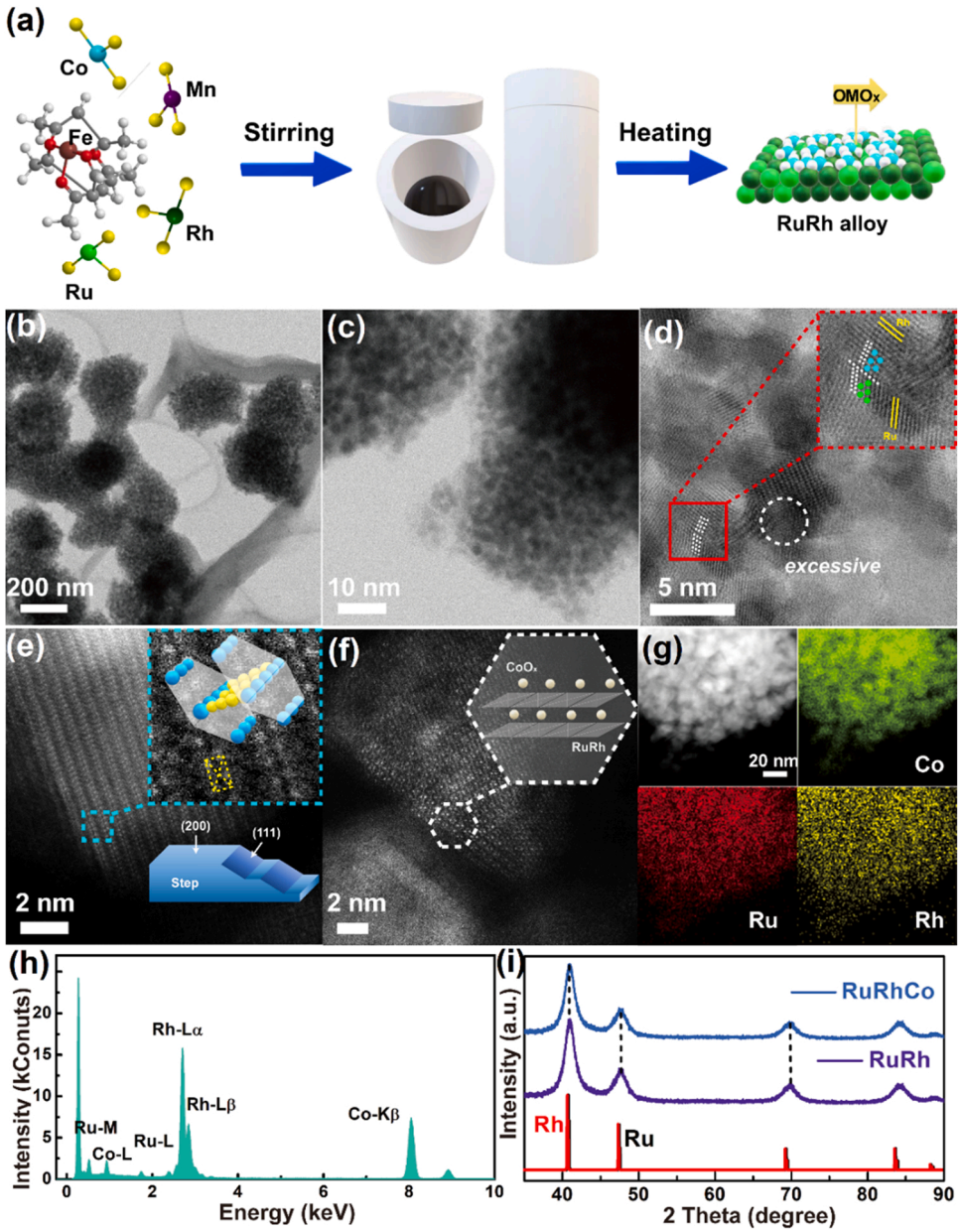

Fig. 2. (a) Scheme of the synthesis of RuRh-OM (OM = Co, Mn, Cr, and Fe) catalysts. (b) TEM images, (c) HRTEM images, and (d) Enlarged HRTEM images of the surface/interfaces of RuRh-Co. (e) and (f) HAADF-STEM images of RuRh-Co. (g) Enlarged HAADF-STEM image and the corresponding EDS mappings of RuRh-Co. (h) SEM-EDS spectrum and (i) PXRD pattern of RuRh-Co.

steps (Fig. 2e and f), which can also boost the catalytic performance. Different element distribution of RuRh-Co can be clearly identified by the EDS linear scan (Fig. 2g), further demonstrating the multipod topology. However, it is noted that no crystal lattice stripe of metallic Co can be found in TEM images due to the ultralow doping. Moreover, the inductively coupled plasma atomic emissions spectrometry (ICP-AES) results reveal that there is very small amount of Co (only about 0.13 wt %) in RuRh-Co (Fig. 2h and Table S1). Thus, as determined by powder X-ray diffraction (XRD) (Fig. 2i), it is entirely explicable there are no peaks for metallic Co, further suggesting that no new crystalline phase was produced in RuRh-Co.

In addition, other ultralow-loaded 3d metal species (0.23 wt% Mn; 2.4 wt% Cr; 1.3 wt% Fe) highly dispersed on RuRh clusters can also be seen (Fig. S3 and Table S1). Further, the surface elements and their valence states in RuRh-OM (M = Co; Mn; Cr and Fe) were further probed by XRD (Fig. S4). With the substituting of 3d metal species, the diffraction peaks of RuRh-OM (M = Mn; Cr and Fe) samples are in consistence with the RuRh-Co without occurrence of new metallic phases.

Through X-ray photoelectron spectroscopy (XPS) analysis, with doping ultralow 3d metal species, the Rh 3d (Fig. 3a) and Ru 3d (Fig. 3b) orbitals move toward higher oxidation state, indicating the lower electron density around Ru (Rh) [29]. Meanwhile, according to the binding energy shift of the characteristic peaks, it can be inferred that the electron transfer occurred between Ru(Rh) and OM, leading to an electron-rich status of OM and an electron-deficient status of Ru(Rh) in the RuRh-OM. Thus, the ΔG decreases, enhancing the catalytic performance of alkaline HOR [30]. The existence of the oxidized species of OM also confirms that they can serve as the OH adsorption sites, boosting the OER process (Figs. S5 and S6). From this, adding OM to RuRh clusters can adjust the *d*-band electron of Ru (Rh), and balance the adsorption and desorption of reaction intermediates, beneficial for the reaction. This conclusion is in good agreement with the DFT calculation results.

To better unveil the oxidation states, the O 1 s XPS of RuRh clusters and RuRh-OM (OM = Co; Mn; Cr and Fe) were further measured. As displayed in Fig. 3c, the peaks located at 530.7, 532.5, and 531.6 eV are attributed to lattice oxygen, hydroxyl group (M-OH), and O_{vac} species, respectively [29,31]. Accordingly, compared with RuRh clusters, there is a large number of oxidized species on the pristine metallic surface and the binding energy (BE) of O suggests that M-O and M-OH coexist on the surface. With the increased proportion of surface OH or M-O species on RuRh-OM, the electron occupations of RuRh-OM orbitals further decrease due to the more loss of electrons, making the *d*-band center of RuRh-Co downshift the most (Fig. 3d), which is also evidenced by the DFT calculations results. Obviously, the introduction of transition metals creates multiple interfaces to diversify the electronic structure of catalysts and then induce inhomogeneity of the adsorption sites.

First, the electrocatalytic performance of RuRh-OM (OM = Co; Mn; Cr and Fe) toward HOR was investigated in a H_2-saturated electrolytes 0.1 M KOH solution [14,32,33]. The iR-corrected linear sweep voltammetry (LSV) curves of RuRh- OM and Pt for HOR are shown in Fig. 4a. The anodic current above 0 V (versus the reversible hydrogen electrode (RHE), same hereafter) is assigned to the oxidation of H_2 [32]. Meanwhile, the RuRh catalyst-modified electrode rapidly loses its activity when the potential is above ~0.35 V because the strong oxophilicity of Ru (Rh) can lead to the formation of oxidation states [19]. The HOR revealed fine structure in the diffusion-limited current range and an asymptotic current decay for potentials above 0.32 V due to the formation of hydroxides on the RuRh-OM catalysts surface and adsorption of anions. However, the RuRh-OM catalysts exhibit higher HOR activity in the whole potential under alkaline conditions compared with RuRh and commercial Pt. Notably, the RuRh-OM catalysts perform the HOR activity of nearly two times even better than Pt on the whole. Fig. 4b displays the polarization curves of RuRh-Co at different rotating speeds from 625 to 2500 rpm. According to the Koutecky-Levich equation, the calculated slope is 6.68 $cm^2\ mA^{-1}s^{-1/2}$ at η = 50 mV, closing to the theoretical value (4.87 $cm^2\ mA^{-1}s^{-1/2}$) for the two-electron transfer of HOR (Fig. S7) [34]. Fig. 4c shows the kinetic current as a logarithmic function versus the potential for samples, and all the curves can be fitted with a value in the range of − 0.1 V~ 0.1 V, indicating a good symmetry

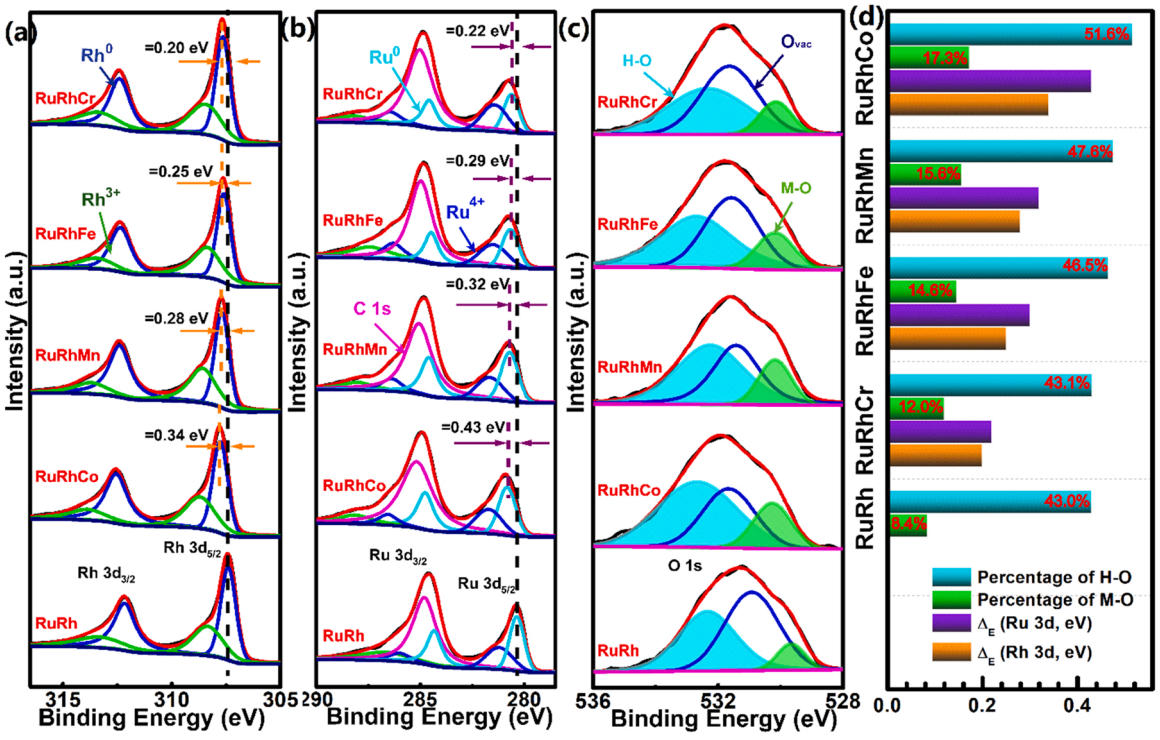

Fig. 3. (a)Rh 3d (the blue line represents Rh^0; green represents Rh^{3+}), (b) Ru 3d (the cyan line represents Ru^0; blue represents Ru^{4+}), and (c) O 1 s core-level XPS spectra of RuRh and RuRh-OM (OM = Co, Mn, Cr, and Fe) catalysts, respectively. (d) comparisons of the amount of OH, M-O, and |Δd| for RuRh and RuRh-OM (OM = Co, Mn, Cr, and Fe) catalysts, respectively.

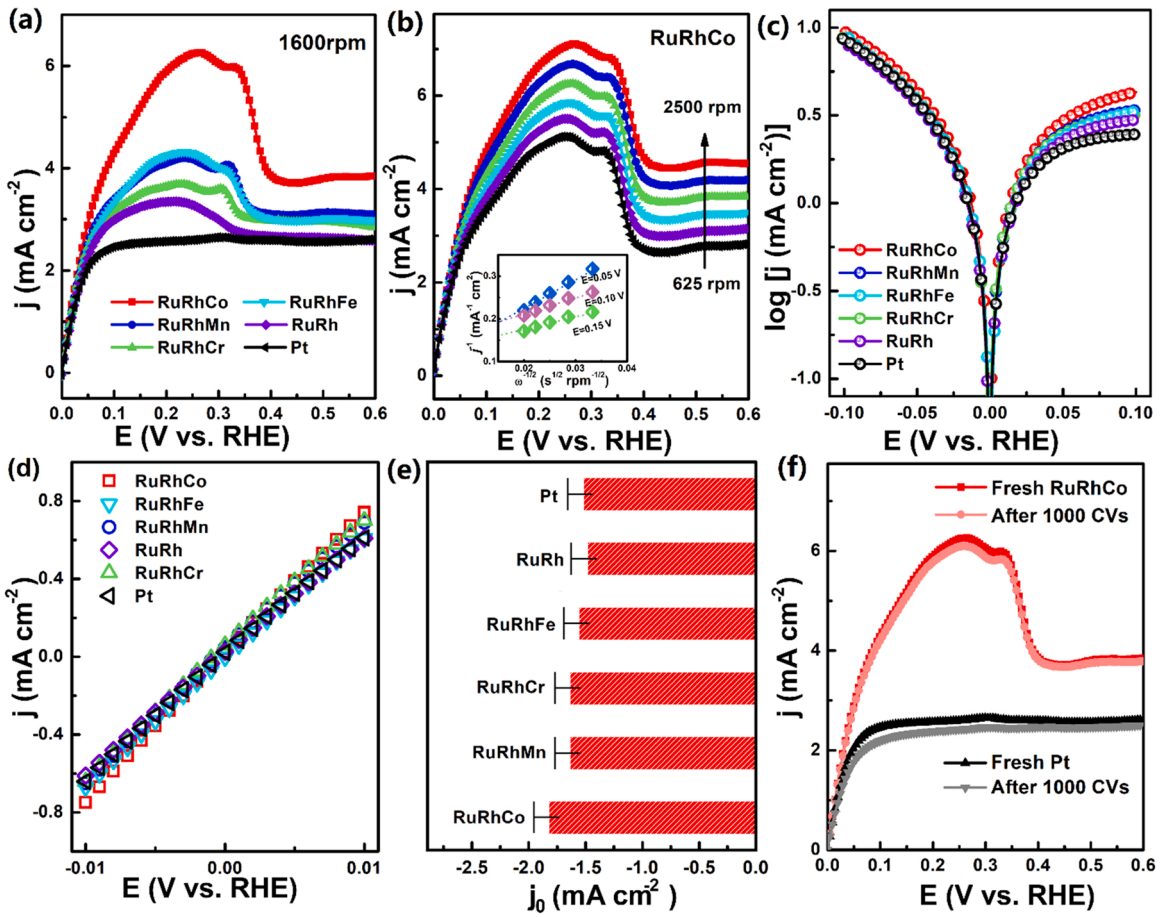

Fig. 4. (a) HOR polarization curves of RuRh, RuRh-OM, and Pt, respectively. (b) Polarization curves of RuRh-Co at different rotating speeds. (c) HER/HOR Tafel plots of kinetic current density on RuRh, RuRh-OM, and Pt, respectively. (d) Micro-polarization region (−10 to 10 mV) of RuRh, RuRh-OM, and Pt catalysts. (e) Exchange current density (j_0) of RuRh, RuRh-OM, and Pt, respectively. (f) Accelerated durability test results of RuRh-Co and Pt.

for the HOR and HER branches.

Further, the corresponding mass activity of RuRh-Co is 11.7 mA/mg at $\eta = 50$ mV, which is the highest among all reported HOR catalysts (Table S2 and S3). In addition, the exchange current density (J_0) was also calculated from kinetic current density data and fitting in the Butler-Volmer equation [35]. As shown in Fig. 4d and e, the value of J_0 for RuRh-Co is 1.91 mA/cm_{disk}^2 at an overpotential of 50 mV, which possesses the highest kinetic current value compared to that of RuRh (1.56 mA/cm_{disk}^2) and commercial Pt (1.60 mA/cm_{disk}^2) catalysts. Overall, as shown in Fig. 4e, the J_0 of RuRh-Co increases by 22% and 19%, compared with that of RuRh and commercial Pt, respectively, in 0.1 M KOH. So, the ultralow-loaded of Co makes it promising for commercial applications (Table S3). In view of the HOR activity and the ΔG (H* and OH*), we have plotted the experimentally obtained j_0 with DFT-calculated ΔG, as illustrated in Fig. S8. Compared with RuRh-OM, the lower HOR performance on RuRh is largely attributed to the weaker-than-optimal OH binding, i.e., the lower oxophilicity. Furthermore, due to the closer ΔG to the linear relation top, RuRh-Co exhibits higher HOR activity than that of all other control samples.

Next, we also examined the stability of the RuRh-Co catalyst. As shown in Fig. 4f, it can be found that RuRh-Co possesses a much less loss in mass activity after 1000 cycles of accelerated tests compared with commercial Pt. In addition, it can work for over 10 h without any noticeable degradation of current density at 0.5 V vs. RHE (Fig. S9). Furthermore, RuRh-Co shows no obvious morphology change after stability test, confirming the superior cycling performance (Fig. S10). Thus, we can conclude that RuRh-Co is an efficient hydrogen oxidation catalyst.

The catalytic performance of RuRh-OM for HER was also evaluated by using the linear scan voltammogram (LSV) with scan rate of 5 mV s^{-1} [36,37], As seen from Fig. 5a. Notably, when scan rate was increased, the double-layer capacitor was highly covered by H_2, causing poor electrical conduction, which synergistically led to the reduced activity compared with that at low scan rate (Fig. S11) [38]. Overall, the overpotential of RuRh-Co at 20 and 50 mA cm^{-2} is 32 and 44 mV, respectively, superior to RuRh-Cr (59 and 79 mV), RuRh-Fe (70 and 91 mV), RuRh-Mn (38 and 52 mV), RuRh (32 and 50 mV), and commercial Pt (44 and 58 mV), and the highest among all reported Ru-based HER catalysts (Fig. 5c, S12 and Table S4) [38]. In addition, It can be seen that, the Tafel slope of 31 mV dec^{-1} (Fig. 5b) for RuRh-Co is close to Pt (35 mV dec^{-1}), suggesting that the HER on RuRh-Co might be proceeded via a Volmer-Tafel mechanism with the step being rate limiting, where the dissociation of H_2O and the recombination of H_{ads} are the RDS for RuRh-Co [39,40]. Meanwhile, from Figs. S13 and 5d, RuRh-Co gives the largest C_{dl} of 101.1 mF cm^{-2}, while RuRh-Fe shows the smallest C_{dl} of 4.2 mF cm^{-2}. Indeed, the large differences in C_{dl} for these catalysts originates from porous multipod-like nanostructure of RuRhCo, which can play an important role on the activity [41]. Furthermore, the fast HER kinetics of RuRh-OM catalysts was further verified measurements [42]. RuRh-Co possesses the smallest R_{ct} of 5.52 Ω (Fig. 5e and S14), we can draw a conclusion that RuRh-Co possesses the fastest electrocatalytic kinetics among the catalysts. Overall, these indicate high electrochemical surface area and fast electrocatalytic kinetics for RuRh-Co, which agrees well with the order of HER activity [42]. Importantly, RuRh-Co displays an excellent stability with a negligible degradation during long-term test (Fig. 5f).

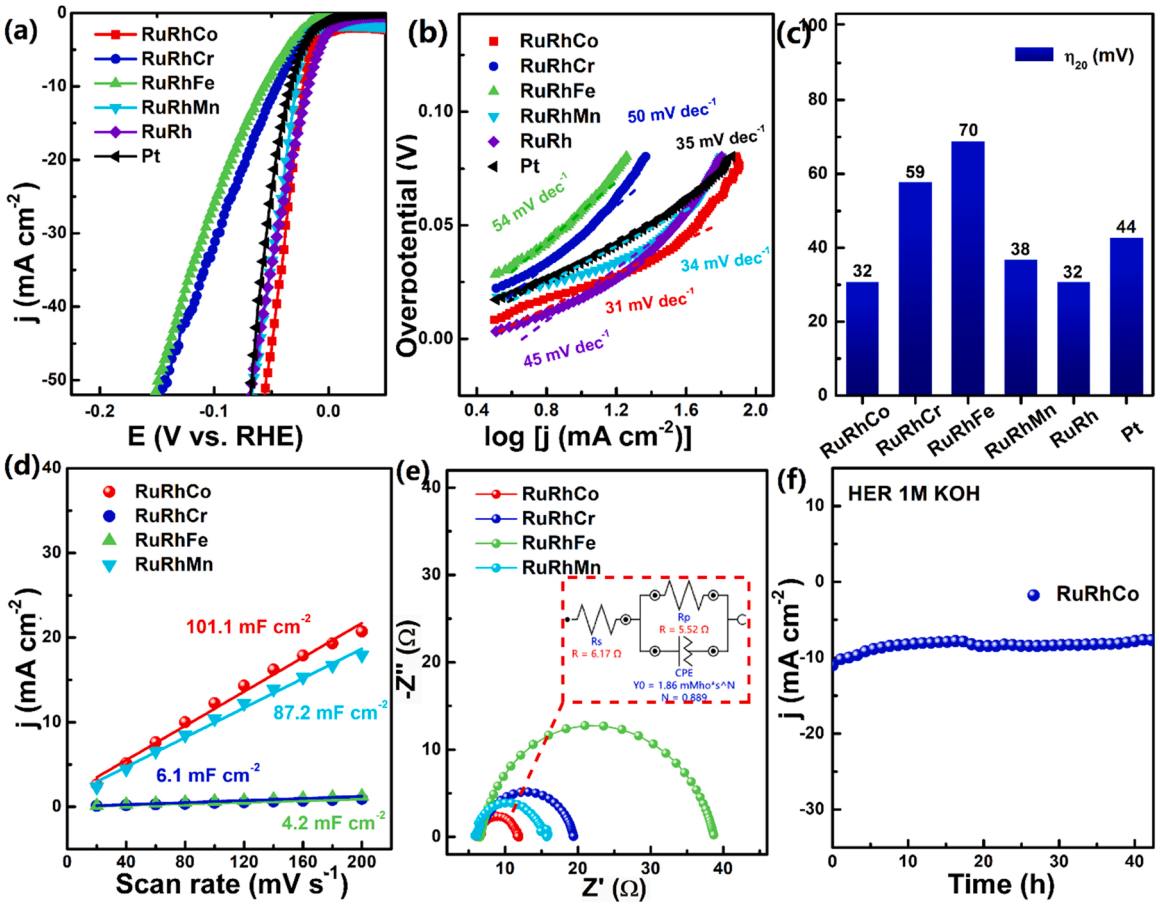

Fig. 5. (a) LSV curves, (b) their corresponding Tafel slopes, and (c) comparisons of overpotential at 20 mA cm^{-2} for RuRh-OM, RuRh, and commercial Pt. (d) Calculated C_{dl} and (e) Nyquist plots for RuRh-OM, RuRh, and commercial Pt, respectively. (f) Time-reliant current density curve for RuRh-Co under an invariant overpotential for 40 h.

Meanwhile, the OER activity in alkaline electrolytes of the samples was also explored [43]. As shown in Figs. S15-S17, RuRh-Co displays greatly improved OER activity with lower overpotentials at the current density of 10 mA·cm^{-2} (324 mV) and outstanding OER stability under 0.1 M KOH. This activity is better than that some other catalysts in the literature (Table S4). On the basis of the HER/OER electrocatalytic activity of RuRh-OM (OM = Co; Mn; Cr and Fe), RuRh-OM catalysts were performed as the anode and cathode catalytic materials for catalyzing full water splitting in a 1.0 M KOH aqueous solution (Fig. S18a). As illustrated in Fig. S18b, on the reference couple (Pt‖IrO_2), to acquire 10 mA cm^{-2}, the cell voltage is 1.52 V. Impressively, at 10 mA cm^{-2}, the cell voltage of RuRh-Co‖RuRh-Co electrodes is as low as 1.49 V, which represents the highest level for overall water splitting (Table S4) [44]. Notably, at larger current density of 50 mA cm^{-2}, RuRh-Co only requires a low cell voltage of 1.57 V, which is the lowest in recent reports (Fig. S18c and Table S4). In addition, the faradaic efficiency for both HER and OER on RuRh-Co is very close to 100%, indicating a high selectivity toward water splitting (Fig. S18e). More importantly, its water splitting electrolysis performs steadily for at least 30 h (Fig. S18f) at 10 mA cm^{-2}.

Based on the above results, our work has been devoted to enhancing the electrochemical reactivity of catalysts in alkaline environments by seeking for the optimized H adsorption and O adsorption energies of ultralow-loaded oxophilic metals (Fe, Co, Ni, etc.) species doped RuRh clusters. To get a more clearly comparison for these catalysts, the relationship involving electrocatalytic activity and overall *d*-band center is also established in the Fig. S19. RuRh-Co with a most optimal *d*-band center, provides the most favorable balance between facilitating H adsorption and O adsorption energies and optimizing in-situ an oxide layer, giving rise to the outstanding activity for alkaline electrocatalysis [21,45].

3. Conclusion

The partial substitution of ultralow oxophilic metal (OM) species in the lattice of RuRh clusters at buried interfaces exhibited particularly high activity for HOR, and unexpected HER/OER and overall water splitting performance in alkaline conditions. We clarified that the enhanced HOR activity on RuRh-OM (OM = Co; Mn; Cr and Fe) mainly results from optimizing H adsorption and O adsorption energies through substituting partial Ru(Rh) clusters at buried atom interfaces with OM species. Meanwhile, as a OH^--adsorption promoter, the in-situ formed oxide layer is also favorable for OER. This study opens new perspectives for significant improvements of rational design of multi-functional electrocatalysts for HER/HOR redox, and even for HER/HOR/OER.

CRediT authorship contribution statement

Yujia Cui: Investigation, Validation, Formal analysis, Data curation, Writing. **Zihan Xu:** Investigation, Validation, Formal analysis, Data curation, Writing. **Ding Chen:** Investigation, Validation, Formal analysis, Data curation. **Tingting Li:** Investigation, Validation, Formal analysis, Data curation. **Hao Yang:** Investigation, Validation. **Xueqin Mu:** Formal analysis, Data curation. **Xiangyao Gu:** Formal analysis, Data curation. **Hong Zhou:** Methodology, Supervision, Project administration, Funding acquisition. **Suli Liu:** Conceptualization,

Methodology, Supervision, Project administration, Funding acquisition, Writing – review & editing. **Shichun Mu:** Methodology, Supervision, Project administration, Funding acquisition, Writing – review & editing.

Declaration of Competing Interest

The authors declare that they have no known competing financial interests or personal relationships that could have appeared to influence the work reported in this paper.

Acknowledgment

This work was supported by the NSFC (21501096, 22075223) and Natural Science Foundation of Jiangsu (BK20150086, BK20201120), Foundation of the Jiangsu Education Committee (15KJB150020), the Six Talent Peaks Project in Jiangsu Province (JY-087) and Innovation Project of Jiangsu Province.

Appendix A. Supporting information

Supplementary data associated with this article can be found in the online version at doi:10.1016/j.nanoen.2021.106579.

References

[1] S.Y. Tee, K.Y. Win, W.S. Teo, L.-D. Koh, S. Liu, C.P. Teng, M.-Y. Han, Recent progress in energy-driven water splitting, Adv. Sci. 4 (2017), 1600337.
[2] A. Kumar, V.Q. Bui, J.S. Lee, A.R. Jadhav, Y. Hwang, M.G. Kim, Y. Kawazoe, H. Lee, Modulating interfacial charge density of NiP_2-FeP_2 via coupling with metallic Cu for accelerating alkaline hydrogen evolution, ACS Energy Lett. 6 (2021) 354–363.
[3] S.Q. Lu, Z.B. Zhuang, Electrocatalysts for hydrogen oxidation and evolution reactions, Sci. China Mater. 59 (2016) 217–238.
[4] Y. Wang, G.W. Wang, G.W. Li, B. Huang, J. Pan, Q. Liu, J.J. Han, L. Xiao, J.T. Lu, L. Zhuang, Pt-Ru catalyzed hydrogen oxidation in alkaline media: oxophilic effect or electronic effect? Energy Environ. Sci. 8 (2015) 177–181.
[5] Z.P. Feng, L. Li, X.Q. Zheng, J. Li, N. Yang, W. Ding, Z.D. Wei, Role of hydroxyl species in hydrogen oxidation reaction: a DFT study, J. Phys. Chem. C. 123 (2019) 23931–23939.
[6] Y. Qiu, L. Xin, Y.W. Li, I.T. McCrum, F.G. Guo, T. Ma, Y. Ren, Q. Liu, L. Zhou, S. Gu, M.J. Janik, W.Z. Li, BCC-phased PdCu alloy as a highly active electrocatalyst for hydrogen oxidation in alkaline electrolytes, J. Am. Chem. Soc. 140 (2018) 16580–16588.
[7] K. Okubo, J.Y. Ohyama, A. Satsuma, Surface modification of Pt nanoparticles with other metals boosting the alkaline hydrogen oxidation reaction, Chem. Commun. 55 (2019) 3101–3104.
[8] X.Y. Tian, P.C. Zhao, W.C. Sheng, Hydrogen evolution and oxidation: mechanistic studies and material advances, Adv. Mater. 31 (2019), 1808066.
[9] L.L. An, X. Zhao, T.H. Zhao, D.L. Wang, Atomic-level insight into reasonable design of metal-based catalysts for hydrogen oxidation in alkaline electrolytes, Energy Environ. Sci. 14 (2021) 2620–2638.
[10] E. Liu, L. Jiao, J.K. Li, T. Stracensky, Q. Sun, S. Mukerjee, Q.Y. Jia, Interfacial water shuffling the intermediates of hydrogen oxidation and evolution reactions in aqueous media, Energy Environ. Sci. 13 (2020) 3064–3074.
[11] Y.C. Yan, H. Shan, G. Li, F. Xiao, Y. Jiang, Y.Y. Yan, C.H. Jin, H. Zhang, J.B. Wu, D. R. Yang, Epitaxial growth of multimetallic Pd@PtM (M = Ni, Rh, Ru) core-shell nanoplates realized by in situ-produced CO from interfacial catalytic reactions, Nano Lett. 16 (2016) 7999–8004.
[12] M.J. Wang, Z.Y. Dang, M. Prato, U. Petrala, I. Infante, D.V. Shinde, L.D. Trizio, L. Manna, Ruthenium-decorated cobalt selenide nanocrystals for hydrogen evolution, ACS Appl. Nano Mater. 2 (2019) 5695–5703.
[13] Q.L. Wu, M. Luo, J.H. Han, W. Peng, Y. Zhao, D.C. Chen, M. Peng, J. Liu, F.M. F. Groot, Y.W. Tan, Identifying electrocatalytic sites of the nanoporous copper-ruthenium alloy for hydrogen evolution reaction in alkaline electrolyte, ACS Energy Lett. 5 (2020) 192–199.
[14] Y.Y. Zhou, Z.Y. Xie, J.X. Jiang, J. Wang, X.Y. Song, Q. He, W. Ding, Z.D. Wei, Lattice-confined Ru clusters with high CO tolerance and activity for the hydrogen oxidation reaction, Nat. Catal. 3 (2020) 454–462.
[15] F.F. Zhang, Y.L. Zhu, Y. Chen, Y.Z.H. Lu, Q. Lin, L. Zhang, S.W. Tao, X.W. Zhang, H. T. Wang, RuCo alloy bimodal nanoparticles embedded in N-doped carbon: a superior pH-universal electrocatalyst outperforms benchmark Pt for the hydrogen evolution reaction, J. Mater. Chem. A 8 (2020) 12810–12820.
[16] D. Cao, H.X. Xu, D.J. Cheng, Construction of defect-rich RhCu nanotubes with highly active Rh_3Cu_1 alloy phase for overall water splitting in all pH values, Adv. Energy Mater. 10 (2020), 1903038.
[17] J.C. Fan, J.D. Wu, X.Q. Cui, L. Gu, Q.H. Zhang, F.Q. Meng, B.H. Lei, D.J. Singh, W. T. Zheng, Hydrogen stabilized RhPdH 2D bimetallene nanosheets for efficient alkaline hydrogen evolution, J. Am. Chem. Soc. 142 (2020) 3645–3651.
[18] Y.-H. Wang, X.-T. Wang, H.J. Ze, X.-G. Zhang, P.M. Radjenovic, Y.-J. Zhang, J.-C. Dong, Z.-Q. Tian, J.-F. Li, Spectroscopic verification of adsorbed hydroxy intermediates in the bifunctional mechanism of the hydrogen oxidation reaction, Angew. Chem. Inter. Ed. 60 (2021) 5708–5711.
[19] S. Qin, Y. Duan, X.-L. Zhang, L.-R. Zheng, F.-Y. Gao, P.-P. Yang, Z.-Z. Niu, R. Liu, Y. Yang, X.-S. Zheng, J.-F. Zhu, M.-R. Gao, Ternary nickel-tungsten-copper alloy rivals platinum for catalyzing alkaline hydrogen oxidation, Nat. Commun. 12 (2021) 2686.
[20] L.J. Gao, Y. Wang, H.B. Li, Q.H. Li, N. Ta, L. Zhuang, Q. Fu, X.H. Bao, A nickel nanocatalyst within a h-BN shell for enhanced hydrogen oxidation reactions, Chem. Sci. 8 (2017) 5728–5734.
[21] H. Xin, A. Vojvodic, J. Voss, J.K. Nørskov, P.F. Abild, Effects of *d*-band shape on the surface reactivity of transition-metal alloys, Phys. Rev. B 89 (2014), 115114.
[22] X.Q. Mu, J.N. Gu, F.Y. Feng, Z.Y. Xiao, C.Y. Chen, S.L. Liu, S.C. Mu, RuRh bimetallene nanoring as high-efficiency pH-universal catalyst for hydrogen evolution reaction, Adv. Sci. 8 (2021), 2002341.
[23] Z.P. Wang, Z.P. Lin, J. Deng, S.J. Shen, F.Q. Meng, J.T. Zhang, Q.H. Zhang, W. W. Zhong, L. Gu, Elevating the *d*-band center of six-coordinated octahedrons in Co_9S_8 through Fe-incorporated topochemical deintercalation, Adv. Energy Mater. 11 (2020), 2003023.
[24] E.S. Davydova, S. Mukerjee, F. Jaouen, D.R. Dekel, Electrocatalysts for hydrogen oxidation reaction in alkaline electrolytes, ACS Catal. 8 (2018) 6665–6690.
[25] D. Strmcnik, M. Uchimura, C. Wang, R. Subbaraman, N. Danilovic, D. van der Vliet, A.P. Paulikas, V.R. Stamenkovic, N.M. Markovic, Improving the hydrogen oxidation reaction rate by promotion of hydroxyl adsorption, Nat. Chem. 5 (2013) 300–306.
[26] S.A. Giles, Y.S. Yan, D.G. Vlachos, Effect of substitutionally doped graphene on the activity of metal nanoparticle catalysts for the hydrogen oxidation reaction, ACS Catal. 9 (2019) 1129–1139.
[27] H.B. Zeng, S.Q. Chen, Y.Q. Jin, J.W. Li, J.D. Song, Z.C. Le, G.F. Liang, H. Zhang, F. Y. Xie, J. Chen, Y.S. Jin, X.B. Chen, H. Meng, Electron density modulation of metallic MoO_2 by ni doping to produce excellent hydrogen evolution and oxidation activities in acid, ACS Energy Lett. 5 (2020) 1908–1915.
[28] F.D. Speck, F.S.M. Ali, M.T.Y. Paul, R.K. Singh, T. Böhm, A. Hofer, O. Kasian, S. Thiele, J. Bachmann, D.R. Dekel, T. Kallio, S. Cherevko, Improved hydrogen oxidation reaction activity and stability of buried metal-oxide electrocatalyst interfaces, Chem. Mater. 32 (2020) 7716–7724.
[29] G. Meng, H. Tian, L.X. Peng, Z.H. Ma, Y.F. Chen, C. Chen, Z.W. Chang, X.Z. Cui, J. L. Shi, Ru to W electron donation for boosted HER from acidic to alkaline on Ru/WNO sponges, Nano Energy 80 (2021), 105531.
[30] B.G. Mao, P.P. Sun, Y. Jiang, T. Meng, D.L. Guo, J.W. Qin, M.H. Cao, Identifying the transfer kinetics of adsorbed hydroxyl as a descriptor of alkaline hydrogen evolution reaction, Angew. Chem. Int. Ed. 59 (2020) 15232–15237.
[31] W.Y. Zhang, Y. Yang, B. Huang, F. Lv, K. Wang, N. Li, M.C. Luo, Y.G. Chao, Y.J. Li, Y.J. Sun, Z.K. Xu, Y.N. Qin, W.X. Yang, J.H. Zhou, Y.P. Du, D. Su, S.J. Guo, Ultrathin PtNiM (M = Rh, Os, and Ir) nanowires as efficient fuel oxidation electrocatalytic materials, Adv. Mater. 31 (2019), 1805833.
[32] Z.Q. Chen, H.B. Wu, W. Guo, C.B. Cao, Z. Chen, Defect enhanced CoP/reduced graphene oxide electrocatalytic hydrogen production with Pt-like activity, Appl. Catal. B: Environ. 265 (2020), 118576.
[33] G.X. Wang, W. Chen, G.L. Chen, J. Huang, C.S. Song, D.L. Chen, Y. Du, C.R. Li, K. K. Ostrikov, Trimetallic Mo-Ni-Co selenides nanorod electrocatalysts for highly-efficient and ultra-stable hydrogen evolution, Nano Energy 71 (2020), 104637.
[34] W.C. Sheng, H.A. Gasteiger, S.-H. Yang, Hydrogen oxidation and evolution reaction kinetics on platinum: acid vs alkaline electrolytes, J. Electrochem. Soc. 157 (2010) 1529–1536.
[35] S.A.S. Machado, L.A. Avaca, The hydrogen evolution reaction on nickel surfaces stabilized by H-absorption, Electrochim. Acta 39 (1994) 1385–1391.
[36] A.S.B.M. Najib, M. Iqbal, M.B. Zakaria, S. Shoji, Y. Cho, X.B. Peng, S. Ueda, A. Hashimoto, T. Fujita, M. Miyauchi, Y. Yamauchi, H. Abe, Active faceted nanoporous ruthenium for electrocatalytic hydrogen evolution, J. Mater. Chem. A 8 (2020) 19788–19792.
[37] Z.P. Lin, B.B. Xiao, Z.P. Wang, W.Y. Tao, S.J. Shen, L.G. Huang, J.T. Zhang, F. Q. Meng, Q.H. Zhang, L. Gu, W.W. Zhong, Planar-coordination $PdSe_2$ nanosheets as highly active electrocatalyst for hydrogen evolution reaction, Adv. Funct. Mater. 31 (2021), 2102321.
[38] W.J. Luo, Y.J. Wang, C.W. Cheng, Ru-based electrocatalysts for hydrogen evolution reaction : recent research advances and perspectives, Mater. Today Phys. 15 (2020), 100274.
[39] Y.Q. Zhao, T. Ling, S.M. Chen, B. Jin, A. Vasileff, Y. Jiao, L. Song, J. Luo, S.Z. Qiao, Non-metal single-iodine-atom electrocatalysts for the hydrogen evolution reaction, Angew. Chem. Int. Ed. 58 (2019) 12252–12257.
[40] H.F. Wang, L.Y. Chen, H. Pang, S. Kaskel, Q. Xu, MOF-derived electrocatalysts for oxygen reduction, oxygen evolution and hydrogen evolution reactions, Chem. Soc. Rev. 49 (2020) 1414–1448.
[41] Z.H. Cheng, Y.K. Xiao, W.P. Wu, X.Q. Zhang, Q. Fu, Y. Zhao, L.T. Qu, All-pH-tolerant in-plane heterostructures for efficient hydrogen evolution reaction, ACS Nano 15 (2021) 11417–11427.
[42] J. Zhu, L.S. Hu, P.X. Zhao, L.Y.S. Lee, K.Y. Won, Recent advances in electrocatalytic hydrogen evolution using nanoparticles, Chem. Rev. 120 (2020) 851–918.

[43] J. Mahmood, F. Li, S.-M. Jung, M.S. Okyay, I. Ahmad, S.-J. Kim, N.P. Park, H. Y. Jeong, J.-B. Beker, An efficient and pH-universal ruthenium-based catalyst for the hydrogen evolution reaction, Nat. Nanotechnol. 12 (2017) 441–446.
[44] H.N. Sun, X.M. Xu, Y.F. Song, W. Zhou, Z.P. Shao, Designing high-valence metal sites for electrochemical water splitting, Adv. Funct. Mater. 31 (2021), 2009779.
[45] E.S. Liu, J.K. Li, L. Jiao, H.T.T. Doan, Z. Liu, Z.P. Zhao, Y. Huang, K.M. Abraham, S. Mukerjee, Q.Y. Jia, Unifying the hydrogen evolution and oxidation reactions kinetics in base by identifying the catalytic roles of hydroxyl-water-cation adducts, J. Am. Chem. Soc. 141 (2019) 3232–3239.

Yujia Cui Yujia Cui majored in Applied Chemistry in Nanjing Xiaozhuang University in 2018. Her main research direction is modification of nanomaterials and electrocatalytic hydrogen production.

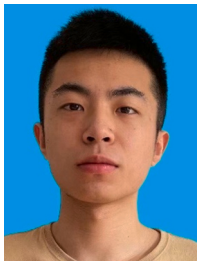

Zihan Xu Zihan Xu majored in Applied Chemistry in Nanjing Xiaozhuang University in 2018. His main research direction is modification of nanomaterials and electrocatalytic hydrogen oxidation.

Ding Chen Ding Chen received his M.D. degree in 2018 from Huainan Normal University in Material Chemistry. Currently he is a doctoral candidate the State Key Laboratory of Advanced Technology for Materials Synthesis and Processing, Wuhan University of Technology. His research interests focus on the rational design and construction nanomaterials and their application in electrocatalysis reactions.

Tingting Li Tingting Li majored in Chemistry Normal in Nanjing Xiaozhuang University in 2018. Her main research direction is modification of nanomaterials and electrocatalytic hydrogen oxidation.

Hao Yang Hao Yang majored in Chemistry Normal in Nanjing Xiaozhuang University in 2018. Her main research direction is modification of nanomaterials and electrocatalytic hydrogen production.

Xueqin Mu Xueqin Mu received her M.D. degree in 2021 from Nanjing Normal University in Inorganic Chemistry. Currently she is a doctoral candidate at the State Key Laboratory of Advanced Technology for Materials Synthesis and Processing, Wuhan University of Technology. Her research interests focus on modification of noble-metal nanomaterials and their application in electrocatalysis reactions.

Xiangyao Gu Xiangyao Gu received his B. D. degree in 2020 from Nanjing Xiaozhuang University in Applied Chemistry. Currently he is a master's research student at the Guangxi Key Laboratory of Low Carbon Energy Materials, Guangxi Normal University. His research interests focus on the Non-noble metal electrocatalysis and diatomic electrocatalysis.

Hong Zhou Hong Zhou graduated from the Department of Chemistry of Anqing Normal University and stayed in the school as a teacher in 1982. He was transferred to Nanjing Xiaozhuang University in 2002 and worked as the dean of the School of Biochemistry and Environmental Science. His research interests focus on organic synthesis, functional complexes and spectral properties of compounds.

Suli Liu Suli Liu received her Ph.D. from the Nanjing Normal University in 2014 and worked as a postdoctoral researcher from 2014 to 2016. She then joined Nanjing Xiaozhuang University and has been a full professor there. She was an academic visitor at the State Key Laboratory of Advanced Technology for Materials Synthesis and Processing, Wuhan University of Technology in 2019–2020. Her research focuses on new energy materials, water splitting electrocatalysts and other related electrochemical catalysis fields.

Shichun Mu Shichun Mu is Chair Professor at Wuhan University of Technology. He received his Ph.D. degree from Chinese Academy of Sciences, China in 2001. Afterwards, he joined the Wuhan University of Technology as a postdoctoral researcher in 2001–2003. Since 2006, he has been a full professor at Wuhan University of Technology. He was an academic visitor at Inorganic Chemistry Laboratory, University of Oxford in 2007–2008. His research focuses on nanocarbon materials, PEM fuel cell/water splitting electrocatalysts and related devices. He has published over 300 peer reviewed papers.